CHLORIDE-PITTING DISSOLUTION OF ROTATING STAINLESS STEEL ELECTRODE IN ACID SOLUTION

N. Sato, T. Nakagawa, K. Kudo and M. Sakashita

Electrochemistry Laboratory, Corrosion Research Center
Faculty of Engineering, Hokkaido University,
Sapporo, JAPAN.

Abstract

Anodic pitting dissolution, pit generation and pit growth of stainless steel at constant potential in sulphuric acid solution containing chloride ion have been investigated by use of rotating electrode. The electrode rotation makes the generation and growth of pits very stable and enables the pit generation frequency and the pitting current from a single pit to be measured potentiostatically. The pits break out at constant frequency and the rate of pit generation is a linear function of the potential, suggesting that the pit generation proceeds electromechanically rather than electrochemically. An incubation time, probably associated with the initial adsorption of chloride ion, is found before the linear pit generation commences, which differs from the induction time for opening an initial pit. The pitting current is in proportion to the area of pit mouth with the current density ($8A/cm^2$) which is independent of the potential, indicating that mass transfer is rate-limiting. The pit grows following a parabolic law and the rate constant is an exponential function of the potential, from which a pit model is proposed in which the transpassive film continuously forming and breaking down on the inner pit surface assumes a high electric field.

1. Introduction

In solutions containing chloride ions passivated stainless steels often corrode locally producing pits on their surface. The chloride pitting corrosion, similarly to any other types of localized corrosion, occurs at random or preferentially at sensitive sites on the metal surface and proceeds only with lack of compositional homogeneity in the environment solution at the pit-sites.

The pitting dissolution of passivated metals, as widely known, consists of two apparently different processes, nucleation and growth of pits. The nucleation (or generation) of pits is a random process occurring on the metal surface and is related to the local breakdown of the passivating film on the surface. It is therefore sensitive to structural and compositional defects — microscopic imhomogeneity — in the passive film or in the metal surface layer, defects which may exist constitutionally or arise from adsorption of chloride ions. On the other hand, the pit growth proceeds by the anodic metal dissolution from the pit and requires condensation of aggressive ions such as chloride and hydrogen ions in the pit — macroscopic imhomogeneity — to break the passive film continuously or to inhibit the formation of passive films on the inner pit surface; Characteristically, it is the pitting dissolution current itself which produces and maintains the macroscopic imhomogeneity necessary to continue the pit growth.

The pit nucleation (or generation) is frequently characterized by a critical pitting potential, defined as the least positive potential at which pits can be generated or grown, and an induction time for pit initiation, defined as the time required before the initial pit breaks out at constant potential after introduction of chloride ions. Some investigators[1-6] have discussed the pitting

potential as the equilibrium potential of the reaction responsible for pit nucleation, while other investigators[7,8] have rather attributed it to the pit propagation process. Similarly, the induction time has frequently been discussed as corresponding to the rate of pit nucleation, although strictly there remains a problem whether it can be related directly to the pit nucleation kinetics.

If we consider the pit nucleation as a random process occurring on the metal surface, the frequency (or rate) of pit generation would be important in understanding the pit nucleation kinetics. Recent studies[9-16] have shown that during pitting at constant potential the number of pits either increases with time or remains almost constant, depending on the time and the potential. In this paper the frequency of pit generation is measured and compared with the induction time for pit initiation.

For the pit propagation previous investigations have presented a number of results which are mainly concerned with the time variation of pitting dissolution current[9-15,17-20] and the growth of pit radius.[9,13,15-17]
Generally, the total pitting dissolution current at constant potential is experimentally given by

$$I = i\,n = t^{x}, \qquad (1)$$

where t is the time after opening an initial pit and n is the number of pits at time t. The pitting dissolution current for a single pit is also given by

$$i = k\,t^{y} \qquad (2)$$

with y, for instance, $y = 0.5$[13] in stagnant solution. For the growth of pit radius recent work has given an experimental equation

of the same type,

$$R = K\, t^{z}, \qquad (3)$$

with exponent z, for instant, $z = 0.5 \sim 1$[13,15,21]. Furthermore, investigations of pit morphology[13,16,18,19,21,22] have shown that, depending on the potential where pitting occurs, the pit grows in the form either of approximate hemi-sphere or of orientational pits, and that the mouth of pits either is open or is closed, presumably also depending on the potential. The closed pit has on its mouth a thin passivated metal cover with a number of small defects. These previous results on pit morphology and pit growth are of value but more is needed to understand the mechanism of pitting dissolution. In this paper experimental results on the pitting dissolution current and the pit growth are presented and discussed in relation to the pit propagation process.

The pitting dissolution or corrosion of stainless steels, as mentioned above, is a strongly localized phenomenon on which the local concentration of aggressive ions on the metal surface has a definite influence. There has been, however, only a few experiments[23] conducted in high speed flow of solutions or with rotating electrodes. This paper describes an experimental study on the anodic pitting dissolution — pit generation and pit propagation — of rotating stainless steel electrode in sulphuric acid solution containing chloride ions.

2. Experimental

2.1. Rotating Electrode

Photo 1 shows the rotating electrode apparatus used, and

Figure 1 gives its schematic representation. The electrode was rotated by a synchronous motor through an urethan rope belt and scored pullys at five different speeds, 450 rpm, 840 rpm, 1450 rpm, 2550 rpm, and 4750 rpm.

Figure 2 gives the dimension of specimen electrode and its holder. The cylindrical specimen electrode, outer diameter 10.4 mm inner diameter 7 mm and length 8 mm, was fastened by a binding bolt to a polyvinyl chloride electrode holder in which a nickel bar with screw coupling on both ends was pluged. Electrical contact with the specimen was made through the central nickel bar connected to the rotating steel shaft to which a copper brush was attached.

The electrolytic cell used is shown in Figure 3. It was a spherical glass vessel of 500 ml with a solution inlet on the upside and an outlet on the bottom, and had an auxiliary platinum plate electrode about 10 cm^2 and a Luggin capillary inserted from its upside.

The electrode potential of the specimen was measured in reference to a saturated calomel electrode, and the anodic polarization was carried out by using a high speed response potentiostat (Nichia HP-E) connected to a current recorder (Hitachi QPD 33).

2.2. Specimen

The stainless steel specimen used was a commercial SUS 27 Steel; C 0.06%, Cr 18.48, Ni 8.95, Si 0.56, Mn 1.02, P 0.020, and S 0.011. The specimen, after mechanically polished with emery papers, was vacuum-annealed at 1100°C for 10 minutes followed by quenching. The surface was then softly polished again using a fine emery paper (0/4), and etched in an acid (6%-HNO_3 10.2 vol %, 46%-HF 2.2 vol %, and H_2O balance) for several minutes immediately

followed by washing in a jet of redistilled water. After dried with benzene and aceton, the specimen was fastened to the electrode holder (Figure 2), and the boundary between the specimen and the holder was sealed using a celluloid lacquer (transparent manicure) to expose the specimen surface about 1 cm^2.

2.3. Solution

The solutions used in this pitting study were 0.2M NaCl plus 0.1M Na_2SO_4 solutions whose pH values were adjusted by adding small amounts of H_2SO_4 at pH 2.3, 3.0, 3.5, 4.0 and 5.0. The solutions used for passivating the specimen were 0.1M Na_2SO_4 solutions of the same pH as above. These solutions were made of analytical grade regents and redistilled water.

2.4. Experimental Procedure

In potentiostatic pitting dissolution experiments, the specimen electrode was passivated at a given potential in 0.1M Na_2SO_4 solution of a given pH for 1 hr, and then the solution was replaced by the test solution (0.2M NaCl+0.1M Na_2SO_4) of the same pH. Immediately after the solution replacement the specimen was polarized again at the same given potential to follow the pitting dissolution. The pitting occurred sometime after the potentiostatic polarization started in the chloride solution, which could be observed by a sudden increase in anodic current. The time required before this sudden current increase appeared was measured as the induction time, τ_1, for opening the initial pit. This induction period of time was followed by a steady pit growth period during which the number of pits as well as the anodic current increased with time. The anodic current during the pit growth was measured as the pitting dissolution current.

In addition, microscopic observations were made to measure the form, figure, radius and depth of pits as functions of time. All the measurements were performed at room temperature ($23 \pm 2^{o}C$) in air-saturated solution.

3. Results

3.1. Effect of Rotation on Pitting Dissolution

Experiments were performed here to investigate the influence of electrode rotation on the chloride pitting potential, on the induction time for pit initiation, and on the time variation of pitting dissolution current of stainless steel. The pitting potential was measured by potential sweep at 6V/hr with specimen electrodes which, prior to potential sweep, were passivated for 1 hr at +0.4V (SCE) in the test solution containing chloride ions. Figure 4 shows the pitting potential and the induction time as functions of the speed of electrode rotation. Within the amount of scatter, the rotation speed is seen to have little influence both on the pitting potential and on the induction time for pit initiation in the range of rotation speed examined.

The rotation speed, however, does affect the initial stage of pitting dissolution. As shown in Figure 5, the pitting dissolution begun with an initial rise of anodic current followed by a steady increase of current which continued until another pit broke out. The initial rise of anodic current was remarkable with the specimen electrode not rotating in stationary solution, while it was only fractional with the rotating electrodes. In the steady pit-growth the pitting dissolution current increased linearly with time, and we obtain the following experimental equation for a single pit,

$$i = k_i (t + a) \qquad (4)$$

where i is the dissolution current, t is the time after opening the initial pit, k_i is the rate of current increase, and a is constant depending on the magnitude of the initial current increase. Constant k_i was nearly independent of the rotation speed, and constant a, although decreasing remarkably by the electrode rotation, was not affected very much by the speed of electrode rotation in the range from 840 rpm to 4750 rpm.

Another effect of rotation found was the deactivation of freshly formed pits, which we often observed when the rotation was set on sometime after the pitting opened in stationary solution. An example of pit deactivation is given in Figure 6, in which the third pit freshly formed in stationary solution is seen to be deactivated by the onset of electrode rotation and only two pits continue to grow.

Figure 7 shows the potentiostatic pitting dissolution current as functions of time at three different speeds. The current-time curve can be seen not to depend very much on the rotation speed but rather to depend on the number of pits being active on the specimen surface.

3.2. Pit Generation

In Figure 7 we have seen that the current-time curve of potentiostatic pitting dissolution of rotating stainless steel electrode consists of straight line segments. Further examples obtained at three different potentials are given in Figure 8. By observing the specimen surface optically, we found that a break in the current-time curve corresponds to a generation of a pit or pits. The current-

time curve, therefore, enabled us to measure the induction time for a series of pits successively breaking out at constant potential, the way of measurements being schematically shown in Figure 9.

To investigate the kinetics of pit generation, we measured a number of current-time curves at different potentials in the solution of pH 3 and estimated the induction time for pits one by one in sequence of pit generation. Results obtained are given in Figure 10. Although the amount of scatter in the induction time is relatively large, it is evident that the pit generation in average proceeds linearly with time and that the more noble potential results in the larger rate (or frequency) of pit generation.
Thus, we obtain the following experimental kinetic equation for pit generation

$$n = k_p (\tau_n - \tau_o) \qquad (5)$$

where n is the number of of pits generated in time τ_n which in turn is the induction time for the n-th pit, k_p is the average pit generation rate (or frequency) at constant potential, and τ_o is a constant.

It is found, as shown in Figure 11, that the rate (or frequency) of pit generation is a linear function of the electrode potential. Thus, we obtain

$$k_p = \beta_p (E-E_{crit}) \qquad (6)$$

where β_p is constant, and E_{crit} is the potential at which the pit generation frequency is expected to be zero. From Figure 11 we estimate $\beta_p = 2.8\ V^{-1} \cdot min^{-1}$ and $E_{crit} = +0.552V$ (SCE) for the solution of pH 3.

Furthermore, it is also found, as shown in Figure 12, that the time τ_o depends exponentially on the electrode potential, and we obtain a Tafel relation

$$E = a_{\tau_o} + b_{\tau_o} \log (1/\tau_o) \qquad (7)$$

where b_{τ_o}, the Tafel slope, is evaluated from Figure 12 b_{τ_o} = 270 mV for the solution of pH 3. Note that τ_o differs from the induction time τ_1 for opening the initial pit and indicates the time at which the linear pit generation commences, which we call here the incubation time. For comparison, Figure 12 also shows $1/\tau_1$ as a function of potential, in which we see τ_o and τ_1 are different in their magnitude and Tafel slope.

3.3. Pitting Dissolution Current

In Figures 7 and 8 we have shown that the dissolution current from steadily growing pits increases linearly with time, and its rate of increase depends on the number of growing pits. The increase rate of the dissolution current can be estimated from the slope of straight line segments in the current-time curves. From some seventy current-time curves measured under various electrode potential and rotation conditions, we estimated the increase rate of the dissolution current in potentiostatic pitting as functions of

the number of active pits, the rotation speed, and the electrode potential. Examples of the results obtained are given in Figure 13. The rate of the current increase is not affected very much by the speed of electrode rotation but is proportional to the number of growing pits. We therefore obtain

$$\frac{dI}{dt} = k_i \quad n \qquad (8)$$

where k_i is the rate of the current increase for a single pit. It is found, as shown in Figure 14, that k_i increases almost exponentially with rise of the electrode potential and its Tafel slope is about 400 mV.

3.4. Pit Form

From microscopic observations we found that almost all the pits formed were approximately hemispherical. Photo 2 and Photo 3 show some micrographs of pits formed on rotating stainless steel electrodes. At higher potentials the pits were always open, while at lower potential — for instant +0.6V(SCE) — the closed pits were formed which had a thin metal cover with a relatively large hole at its centre and a number of small holes distributed at random.

Furthermore, we measured using a microscope the radius R and depth H for a number of pits formed at various potentials. Some results obtained with pits formed at two different potentials are given in Figure 15, from which it is clear that the pits are not exactly hemispherical and increase in the ratio H/R as they grow.

3.5. Pit Growth

To follow the steady pit growth we measured the radius of pits

formed at various constant potentials as functions of time after they broke out. Figure 16 gives an example of the results obtained, from which it is apparent that the rate of the pit growth at constant potential is almost independent of the speed of electrode rotation and that the pit radius in average increases following a nearly parabolic scheme.

$$R = k_R \sqrt{t} \qquad (9)$$

This relation can be examined in Figure 17, where the area of pit mouth, $S_m = R^2$, is plotted against time. From this result together with other results obtained at different potentials, we obtain the following experimental equation

$$S_m = k_s \quad t \qquad (10)$$

where k_s is the rate of pit growth in area of the pit mouth. These results on the time variation of the pitting radius and surface are in agreement with the result reported by Rosenfeld and Danilor[12] who made measurements with artificial pits.

It is also found, as shown in Figure 18, that k_s is an exponential function of the potential with a Tafel slope about 400 mV. This Tafel slope should of course be equal to the Tafel slope for k_i given in Figure 14.

4. Discussion

4.1. Pitting Dissolution of Rotating Electrode.

The test electrode rotating at 450 - 4700 rpm in the test solution induces turbulent flow of solution on the electrode surface, since its Reynolds number Re = $2\text{-}40 \times 10^3$ is beyond the laminar flow region. The test solution contained a saturated amount of dissolved oxygen, which however would have little effect on the pitting dissolution current in the potential range examined because practically no cathodic reduction of oxygen occurs at potentials more positive than +0.6V(SCE)[24].

In Figure 4 we have shown that there is almost no influence of high speed flow of solution both on the pitting potential and on the induction time for pit initiation. We see from these facts that any mass transfer does not control the pit nucleation process and hence that the pit nucleation is a process which occurs in the passivating film itself.

As shown in Figure 5 and 6, the pit growth in an initial stage was more remarkable in stagnant solution than in moving solution, and the stability of freshly formed pits depended on mass transfer in the solution outside the pits to greater extent in stagnant solution than in turbulent flow. Before the steady pit growth started, the pitting dissolution current increased to a certain value given by $k_i a$ in (4) and hence the pit grew to a certain size depending on the solution flow. This critical pit size can be evaluated from $k_i a$, provided that the pitting current density i_o at the pit mouth is known. From Figure 5, for examples, we estimate using i_o = $8 A/cm^2$ (Table 1) the critical pit radius to be 42 μ in stagnant solution, 20 μ at 840 rpm and 10 μ at 2550 rpm. Beyond the critical size the pit grew steadily at a constant rate which, although depending on the potential, was not affected very much by the speed of

electrode rotation, as shown in Figure 5, 7 and 13. It appears therefore that in the steady pit growth the stability and the growth rate of pits are no longer dependent on the solution flow outside pits but rather controlled by the concentrated solution inside pits upon which the electrode rotation would have little effect.

4.2. Pit Generation

In Figure 9 we have shown that the rotation of specimen electrodes enables us to measure not only the induction time for opening the initial pit but also the rate of pit generation by simply observing the time variation of anodic current. This would provide a convenient method for measuring the pit generation rate on passivated metals at constant potential.

For stainless steel we have seen in Figure 10 that in high speed flow of solution the number of pits increases linearly with time at constant potential. The rate of pit generation is thus given from (5) by

$$k_p = (\partial n / \partial \tau_n)_E$$

In recent work[9,11,13], stainless steel, as well as iron, even in stagnant solution showed a linear kinetics of pit generation at constant potential, with a few exceptions[9,10,12] showing non-linear pit generation probably as a result of the interaction between pits which would become effective with increase of pit density.

It is to be noted that the pit generation rate k_p differs from the inverse of the induction time $1/\tau_1$, the rate of opening the initial pit. The relation between them is obtained from (5) as

$$\frac{1}{\tau_1} = \frac{k_p}{(1 + k_p \tau_o)} \qquad (11)$$

We thus see that $1/\tau_1$ would approximate the rate of pit generation k_p, only if τ_o be very close to zero. Experimentally, however, as shown in Figure 10 for examples τ_o was fairly apart from zero and hence $1/\tau_1$ could not represent the rate of pit generation, i.e. the steady rate of pit nucleation.

In Figure 10 we have seen that τ_o is the time at which the linear pit generation process might start after introduction of chloride ions. This is the incubation time associated with opening the linear pit generation, and may be explained as the time required before the passivating film is in equilibrium or steady state with respect to the adsorption of chloride ion. To explain τ_o we give Figure 19, which shows schematically the change that would occur in the passivating film on stainless steel in contact with solution containing chloride ions. Evidently, we see that $1/\tau_o$ corresponds not to the kinetics of the film breakdown or pit generation but rather to the rate of chloride ion adsorption on or incorporation to the passivating film. As shown in Figure 12, $1/\tau_o$ increased exponentially with the potential in agreement with a Tafel relation, from which it is suggested that an electrochemical process such as chloride ion adsorption is responsible for $1/\tau_o$.

Furthermore, from the fact that the rate or frequency of pit generation k_p depends linearly with the potential (Figure 11), we see that the process which controls the rate of pit generation, i.e.

the frequency of film breakdown, is not an electrochemical reaction but rather an electrical process such as a mechanical film breakdown due to the electrostriction pressure, as previously proposed by one of the authors[25]. We need, of course, further experiments before clarifying the mechanism of pit generation and film breakdown. However, any further study on the kinetics of pit generation should take into account the difference in physical meaning between the induction time τ_1, the incubation time τ_0, and the pit generation rate k_p described above.

4.3. Pitting Dissolution Current

In Photo 2 we have shown that all the pits except those formed at +0.6V are of the open type and their mouth are approximately circular. At +0.6V the pits were of the closed type with a round, thin and porous metal cover. The closed pits on stainless steels have often been observed by other workers[13,19,22] to form at potentials rather close to the critical pitting potential. From examining the potentials for open and closed pits we see that there might be a boundary potential separating the potential regions for the two types of pit, as suggested by Hoar[5] and Bianchi.[26] We here discuss the pitting dissolution current from the open pit.

During the study growth the pitting dissolution current from a single pit was a linear function of time (Figure 9 and 13) and also the area of the pit mouth increased linearly with time (Figure 17). From these results we see that the pitting dissolution current is in proportion to the area of pit mouth.

The metal ion transfer across the pit mouth can generally be given by the flux

$$\Phi = \left(D_M \frac{d C_M}{dx} + zu C_M \frac{d\varphi}{dx} + w C_M\right) S_m \qquad (12)$$

where C_M is the concentration of metal ion at the pit mouth, D_M the diffusion coefficient, z the ionic valency, u the ionic mobility, $d\varphi/dx$ the potential gradient, w the flow rate of solution across the pit mouth. The first term in (12) represents the diffusion, the second the field assisted ion migration, and the third the convection. In our experiments the last term in (12) might be negligibly small because the pit depth is almost the same as or less than the thickness of the solution boundary layer or the diffusion layer on the metal surface on which $w = 0$. Assuming that $D_M = 1 \times 10^{-5}$ cm/sec, $u = 5.10^{-4}$ cm^2/sec.V, $d\varphi/dx = 0.1$ V/cm, and the diffusion layer thickness $\delta = 0.005$ cm, we estimate the first term in (12) to be $0.002\ C_M$ and the second to be $0.0001\ C_M$, from which it is suggested that the diffusion is predominant.

Equation (12) may be written as

$$\Phi = k\ Sm \qquad (13)$$

where k is the flux density of transferring metal ion at the pit mouth. Furthermore, the material balance with respect to the metal ion gives

$$\Phi = (i/zF) - C_M\ (dV/dt) \qquad (14)$$

where the first term represents the rate of metal dissolution inside

the pits and the second the rate of accumulation of metal ion in the pit, V being the volume of pit. Since $i = (zF\rho / M)(dV/dt)$, we obtain from (14)

$$\Phi = (i/zF)(1 - M C_M/\rho) \qquad (15)$$

where M and ρ are the molecular weight and the density of the metal, respectively. Note that we have here assumed that the concentration of metal ion in the pit, C_M, is unchanged during the pitting dissolution; C_M would be very large and close to the saturation concentration for metal salts.

From (13) and (15),

$$i = \frac{zF\ k\ S_m}{1 - (M C_M/\rho)} = i_o S_m \qquad (16)$$

and hence

$$i_o = \frac{zFk}{1-(M C_M/\rho)} \qquad (17)$$

These two equations indicate the pitting dissolution current to be proportional to the area of the pit mouth S_m and the current density i_o to be determined by the metal ion transfer across the pit mouth.

Our experiments can estimate the current density i_o at the pit mouth. From (4) and (10), and neglecting the term $k_i a$ in (4) because it vanishes at high speed flow of solution, we obtain,

$$i = (k_i/k_s)\ S_m \qquad (18)$$

and hence

$$i_o = k_i/k_s \qquad (19)$$

Experimentally, as shown in Figure 20, the ratio k_i/k_s was always constant irrespective of the potential and of the solution pH. Table 1 summarizes k_i, k_s, and i_o evaluated at various potentials and solution pH. As an average, we obtain

$$i_o = 8\ A/cm^2 \qquad (20)$$

The fact that i_o was almost independent of the speed of electrode rotation is readily explained by the turbulent flow which provides a nearly constant thickness of the diffusion layer on the metal surface.

It is remarkable that the current density i_o is not affected by the potential and the solution pH. From this we see, as suggested before, that the mass transfer of metal ion across the pit mouth is controlled mainly by the diffusion. Consequently, k in (12) is approximated by $D_M(C_M/\delta)$, and from (17) we obtain

$$C_M = \frac{i_o}{zF(D_M/\delta) + i_o(M/\rho)} \qquad (21)$$

Rough estimate using $D_M = 1 \times 10^{-5}$ cm/sec and $\delta = 0.001 \sim 0.005$ cm gives

$$C_M \fallingdotseq 4 \sim 20 \text{ mol}/\ell \ , \qquad (22)$$

from which it is suggested that the concentration of metal ion in the pit is in saturation or in supper saturation with metal salts.

In recent work[7,10,19], the pitting current density at pit mouths on stainless steels in stagnant solution was measured and found to increase with the potential in the potential range less positive than that examined in this work. In Figure 21 the current density i_o estimated by other workers is compared with ours. Note that at potentials less positive than +0.6V the closed pits are formed, while the pits formed at more positive potentials are open. At this stage, however, it is not made clear whether the decrease of i_o with descending the potential results from the resistance in mass transfer across the pit cover or from the pitting dissolution mechanism that might differ depending on the potential region.

Nevertheless, from our results it is evident that in the potential region where the current density i_o is constant the pitting dissolution proceeds in much the same mechanism as that of electropolishing or electrobrightening.

4.4. Form of Pits

In Figure 15 we have shown that the form of pits is not exact hemisphere but changes in the ratio of depth to radius H/R during pit growth. Now, express the volume of a pit as

$$v = (2/3)\pi R^3 \alpha \qquad (23)$$

where α is a correction factor for deviation from hemisphere, and assume α to be given by $\alpha = \alpha_o R^x$ as a function of R, then we have

$$V = (2/3)\pi \alpha_o R^{(3+x)} \qquad (24)$$

Since our experiments gave $R = k_R t^{0.5}$ as presented by (9), we obtain the pit volume as a function of time

$$V = (2/3)\pi \alpha_o k_R^{(3+x)} \quad t^{(1.5+0.5x)} \qquad (25)$$

The pitting dissolution current from a single pit therefore is given by

$$i = \frac{zFM}{\rho} \cdot \frac{dV}{dt} = K' \ t^{0.5+0.5x} \qquad (26)$$

Comparing (26) with the experimental results given by $i \approx k_i t$, we obtain $x \approx 1$, and hence the correction factor α is nearly proportional to the pit radius. This is in qualitative agreement with the results shown in Figure 15.

4.5. Pit Growth Kinetics

In the first approximation we take the radius of the pit mouth,

R, as an representative dimension of the pit and the rate of its increase, dR/dt, as an representative rate of pit growth.
Then, from our experimental results given by (9) and (10) we obtain for the rate of pit growth

$$v = \frac{dR}{dt} = \frac{k_R^2}{2R} = \frac{k_s}{\pi} \cdot \frac{1}{2R} \qquad (27)$$

Obviously, this is a parabolic rate equation in which the rate is inversely as the pit dimension, and suggests that the rate is controlled by the diffusion of dissolving metal ion through the pit.

In order to explain the experimental results with respect to the rate constant $k_R^2 (= k_s/\pi)$ and its potential dependence given in Figure 18, we now postulate a pit model (Figure 22) in which the inner pit surface has a superficial oxide film forming and breaking down continuously during the pit growth, the thickness of which is of the same order as of the passivation film; Such a film may be called the transpassive film or electropolishing film. Furthermore, we assume that the ionic diffusion in the solution within the pit is linear under the aiding field $\Delta\phi_R/R$ which is relatively small,

$$v(R) = v_o' \frac{\Delta\phi_R}{R} , \qquad (28)$$

while in the surface oxide film non linear diffusion of the Cabrera and Mott type[27] is limiting the ion migration rate under the very strong aiding field $\Delta\phi_d/d$ of the order of 10^{-6}V/cm

$$v(d) = v_o \exp\left(\frac{\beta \Delta\phi_d}{d}\right) \qquad (29)$$

where d is the thickness of the surface film, $\Delta\phi_d$ and $\Delta\phi_R$ are the potential difference across the film and in the pit solution, respectively.

At the steady state where v = v (R) = v (d), we obtain from (27), (28) and (29)

$$k_s = \pi k_R^2 = 2\pi v_o R \exp\left(\frac{\beta \Delta\phi_d}{d}\right) \qquad (30)$$

The potential difference $\Delta\phi$ between the metal and the solution outside the pit, to which the electrode potential is directly related, is given by the sum of $\Delta\phi_d$ and $\Delta\phi_R$. If $\Delta\phi_d \gg \Delta\phi_R$ as it would be in actual pitting dissolution, $\Delta\phi_d$ approximates $\Delta\phi$ and hence (30) gives

$$k_s = 2\pi v_o R \exp\left(\frac{\beta \Delta\phi}{d}\right) \qquad (31)$$

The pre-exponential factor ($2\pi v_o R$) can be assumed to be almost constant compared with the exponential term. Evidently, therefore, this equation explains the experimental fact given in Figure 18 that k_s increases exponentially with the potential holding a Tafel relation.

5. Conclusion

The following conclusion can be drawn from this study:

(1) The high speed rotation of electrode makes the pit growth very stable and enables the pitting dissolution current from a single pit to be measured. But little does it affect the pitting potential and the pit generation frequency.

(2) By use of rotating electrode it is made possible to measure readily the induction times for successively opening pits and hence the frequency of pit generation at constant potential.

(3) Potentiostatically, pits break out at a constant frequency and hence the number of pits n is a linear function of time τ_n,

$$n = k_p (\tau_n - \tau_o)$$

where the rate (or frequency) of pit generation k_p increases linearly with the potential.

(4) From the linear dependence of k_p on the potential, we see that the process controlling the pit generation is electrical or electro-mechanical rather than electrochemical

(5) An incubation time τ_o is required for the onset of the linear pit generation, which obviously differs from the induction time τ_1 for opening an initial pit and which may be associated with establishing chloride ion adsorption equilibrium on or in the passivation film.

(6) The pitting dissolution current from a single pit is in proportion to the area of pit mouth, and the current density is constant (i_o = 8A/cm^2) irrespective of the potential (+0.60V ~ +1.00V, (SCE)), indicating that the mass transfer of dissolving metal ion through

the pit mouth is rate limiting. The metal ion concentration in the pit solution, estimated from i_o = 8A/cm^2, is so large (4 ~ 20 mole/l) that a polymer of metal chloride or other metal salts can be deposited. We see therefore that the pitting dissolution in the potential range examined is similar to the electropolishing dissolution.

(7) The pit grows following a parabolic law in which the rate decreases inversely as the pit dimension, and the parabolic rate constant increases with the potential obeying a Tafel relation. From this we see that the field-assisting ionic migration through the pit is rate-limiting, and propose a pit model in which a thin barrier layer, continuously forming and breaking down on the inner pit surface, assumes a high electric field; Such a layer may be called the transpassive film or electropolishing film.

(8) The form of pits is approximately hemi-spherical but the ratio of its depth to radius increases as the pit grows.

References

1) Ja.M. Kolotyrkin: Corrosion, 19, 261t (1963).

2) H.P. Leckie and H.H. Uhlig: J. Electrochem. Soc., 113, 1262 (1966).

3) K.J. Vetter: Ber. Bunsenges. phys. Chem., 69, 683 (1965); K.J. Vetter and H.-H. Strehblow: Ber. Bunsenges. phys. Chem., 74, 449, 1024 (1970).

4) H. Kaesche: Z. physik. Chem.(N.F.), 34, 87 (1962); 26, 138 (1960).

5) T.P. Hoar: Corrosion Sci., 7, 341 (1967).

6) D.A. Vermilyea: J. Electrochem. Soc., 118, 529 (1971).

7) W. Schwenk: Corrosion Sci., 3, 107 (1963); Corrosion, 20, 129t (1964).

8) H. Rickert and G. Holzäpfel: Werk. u. Korr., 17, 376 (1966); Ber. Bunsenges. phys. Chem., 70, 171 (1966).

9) G. Herbsleb und H.-J. Engell: Z. phys. Chem., 215, 167 (1960).

10) Z. Szkarska-Smialowska and M. Janik-Czachor: Brit. Corrosion J., 4, 138 (1969).

11) J. Tousek: Collection Czechoslov. Chem. Commun., 35, 774 (1970); Werks. u. Korr., 21, 21 (1970).

12) V. Ashworth, P.J. Boden, J.S.Ll. Leach and A.Y. Nehru: Corrosion Sci., 10, 481 (1970).

13) I.L. Rosenfeld and I.S. Danilov: Corrosion Sci., 7, 129 (1967).

14) I. Garz., H. Worch and W. Schatt: Corrosion Sci., 9, 71 (1969).

15) G. Herbsleb: Werkst. u. Korr., 17, 649 (1966).

16) N. Ohtani, K. Aihara and S. Takamoto: J. Japan Inst. Metals, 33, 377 (1969).

17) H.-J. Engell und N.D. Stolica: Z. phys. Chem., (N.F.), 20, 113, (1959); Arch. Eisenhuttenwes. 30, 239 (1959).

18) K.J. Vetter und H.-H. Strehblow: Ber. Bunsenges. physik. Chem., 74, 1024 (1970).

19) T. Yoshii and Y. Hisamatsu: J. Japan Inst. Metals, 35, 151 (1971), 34, 1207 (1970).

20) T. Suzuki and Y. Kitamura: Denki Kagaku, 38, 526 (1970); Corrosion Eng. Japan, 18, 100 (1969), 17, 535 (1968).

21) Y. Matsumura and Y. Hisamatsu: 17th Annual Symposium on Corrosion and Protection in Japan (1970), Extended Abstract, p.377; T. Yoshii, Y. Hisamatsu and Y. Matsumura: J. Japan Inst. Metals, 35, 633 (1971).

22) P. Forchhammer und H.-J. Engell: Werks. u. Korr., 20, 1 (1969).

23) I.V. Riskin and A.B. Turkovskaya: Zashch. Metal., 5, 443 (1969).

24) G. Okamoto, T. Shibata and N. Sato: Annual Rep. The Asahi Glass Foundation for the Contribution to Industrial Technology, 15, 207 (1969).

25) N. Sato: Electrochimica Acta, 16, in press (1971).

26) G. Bianchi, A. Cerquetti, F. Mazza, S. Torchio: Corrosion Sci., 10, 19 (1970).

27) N. Cabrera and N.F. Mott: Rep. Progr. in physics, 12, 163 (1949).

Figure 1. Rotating electrode apparatus.

Figure 2. Specimen electrode.

Figure 3. Cell.

Figure 4. Effect of rotation speed on the pitting potential (A) and the induction time (B) for opening an initial pit on stainless steel electrode in 0.2M NaCl + 0.1M Na_2SO_4 solution.

E_{pit} was measured by potential sweep at 6V/hr from a starting potential +0.4V (SCE) where the specimen, prior measurement, was potentiostatically passivated for 1 hour in the test solution. The specimen for measuring τ_1 was passivated 1 hour at 0.6V (SCE) in 0.1M Na_2SO_4 solution of pH 3 before introduction of chloride ion.

Figure 5. Time variation of pitting dissolution current at constant potential (+0.6V) after opening the initial pit on stationary and rotating stainless steel electrodes in solution of pH 3 (0.1M Na_2SO_4 + 0.2M NaCl). Specimens were potentiostatically passivated at +0.7V for 1 hour in 0.1M Na_2SO_4 solution of pH 3 prior to introduction of chloride ions.

Figure 6. Time variation of pitting dissolution current of a stainless steel electrode at a constant potential in solution of pH 3 (0.1M Na_2SO_4 + 0.2M NaCl), illustrating deactivation of a pit by rotation. Rotation was set on after the third pit opened and the most fresh pit was deactivated by rotation. n denotes the number of growing pits. Dotted lines indicate expected curves along which the anodic current would increase under stationary condition if no further pit generation occurred.

Figure 7. Time variation of pitting dissolution current at constant potential after opening the initial pit on stainless steel electrode rotating at different speeds in solution of pH 3 (0.1M Na_2SO_4 + 0.2M NaCl). n denotes the number of growing pits.

Figure 8. Time variation of pitting dissolution current at three different potentials of rotating stainless steel electrode in solution of pH 3 (0.1M Na_2SO_4 + 0.2M NaCl) after introduction of chloride ion.

Figure 9. Schematic representation of current time curve of potentiostatic pitting dissolution of rotating stainless steel electrode by chloride ions. τ_n denotes the induction time required for the n-th pit to break out.

Figure 10. Induction time τ_n for opening pits in sequence as a function of pit number n at three different potentials in solution of pH 3 (0.1M Na_2SO_4 + 0.2M NaCl). The open circule is the mean value based on N measurements and the vertical line segment is the standard deviation.

Figure 11. Effect of the potential on the pit generation rate. The plot is based on the results given in Figure 10.

Figure 12. Effect of potential on the incubation time τ_o for onset of linear pit generation. Plot is based on the results given in Figure 9 and the broken line indicated τ_1 for comparison.

Figure 13. The rate of current increase at constant potential during pit growth as a function of the number of growing pits on rotating stainless steel electrode in solution of pH 3 (0.1M Na_2SO_4 + 0.2M NaCl).

Figure 14. Potential dependence of k_i

$$k_i = \left[d (\partial I / \partial t)/dn \right]_E$$

Figure 15. The ratio of depth H to radius R as functions of pit radius R for a number of pits formed at +0.7 V and +0.8 V in solution of pH 3 (0.1M Na_2SO_4 + 0.2M NaCl).

Figure 16. Growth in radius of pit mouth at constant potential on rotating stainless steel electrode in solution of pH 3 (0.1M Na_2SO_4 + 0.2M NaCl).

Figure 17. Growth in area of pit mouth at constant potential on rotating stainless steel electrode in solution of pH 3 (0.1M Na_2SO_4 +0.2M NaCl).

Figure 18. Potential dependence of k_s.

$$k_s = \left(\partial S_m / \partial t \right)_E$$

Figure 19. Scheme for the initial stage of pitting.

Figure 20. Relation between k_i and k_s.

Figure 21. Pitting current density at pit mouth.

- ○ Present work
- ● 18Cr-8Ni, 1 n H_2SO_4 + 0.5M NaCl, stagnant solution by Yoshii and Hisamatsu[19].
- ▲ 16Cr, 0.7N Na_2SO_4 + 0.7N NaCl, stagnant solution, by Szklarska-Smialowska and Janik-Czachor[10]
- ■ 18N-10Cr, 1 N H_2SO_4 + 1 M NaCl, stagnant solution, by Schwenk[7].

Figure 22. A proposed model and potential distribution for pit.

Photo 1. Rotating electrode apparatus.

Photo 2. Microscopic view of pits formed on rotating stainless steel electrode in solution of pH 3 (0.1M Na_2SO_4 + 0.2M NaCl).

Photo 3. Microscopic view of pits formed on rotating stainless steel electrode in solution of pH 3 (0.1M Na_2SO_4 + 0.2M NaCl).

Table 1. Rate of pitting current increase for a single pit, pit growth rate in area of pit mouth, and pitting current density at pit mouth.

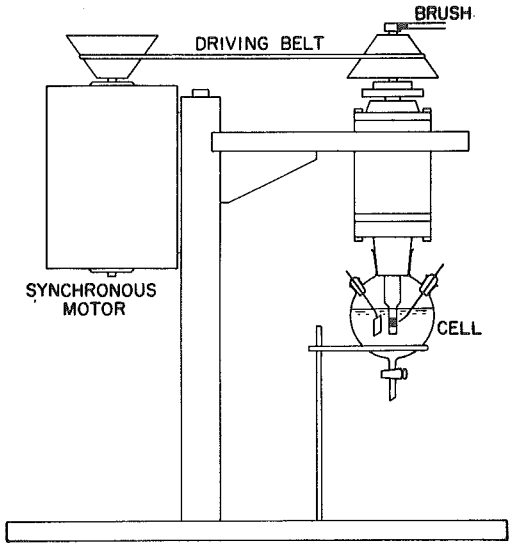

Fig. 1.

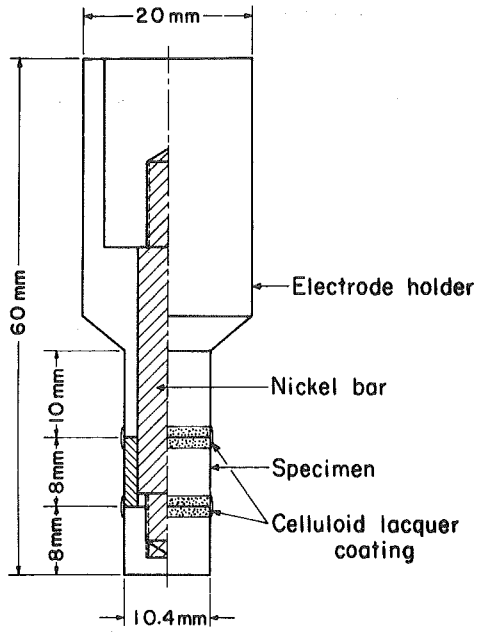

Fig. 2.

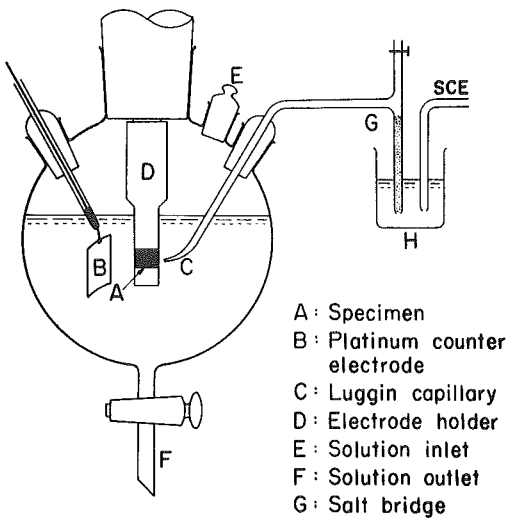

Fig. 3.

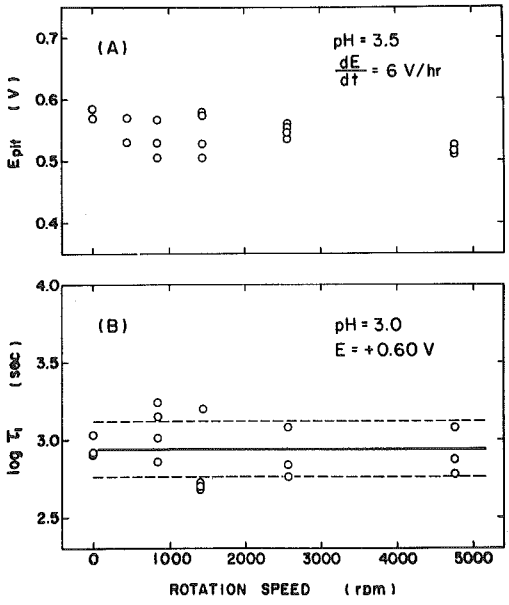

Fig. 4.

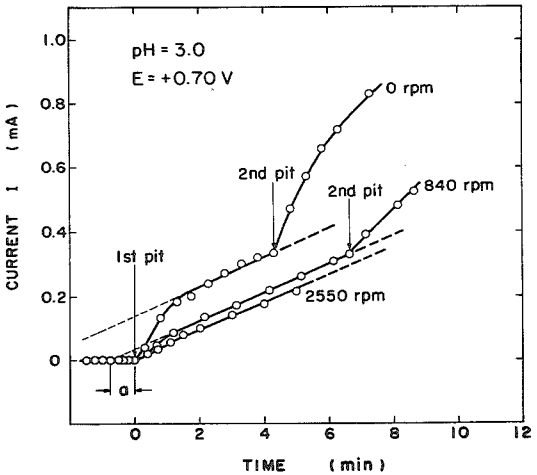

Fig. 5.

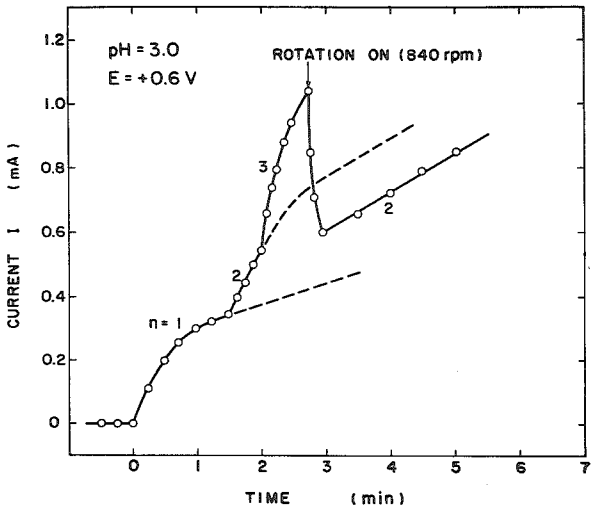

Fig. 6.

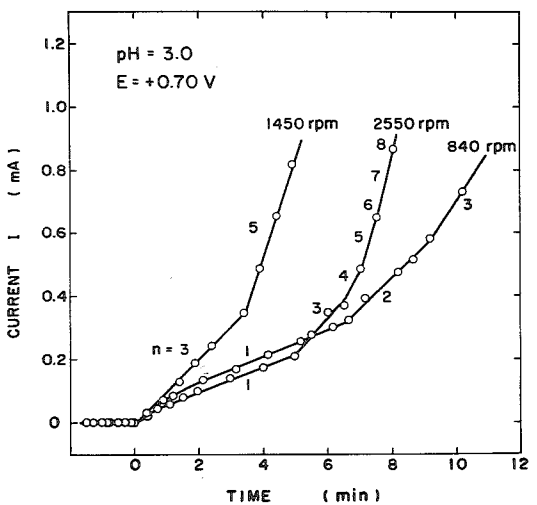

Fig. 7.

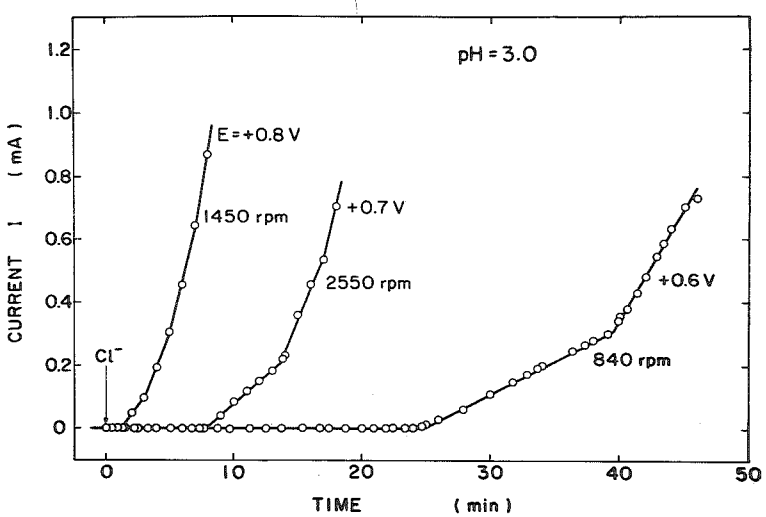

Fig. 8.

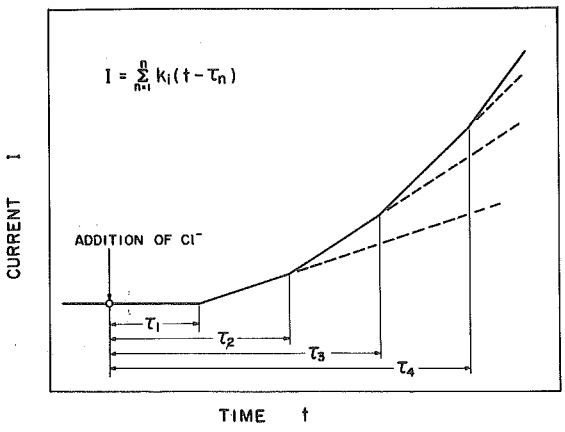

Fig. 9.

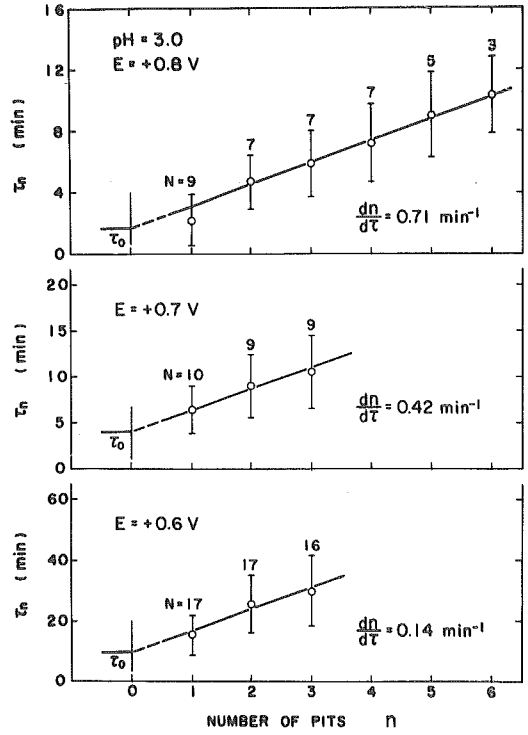

Fig. 10.

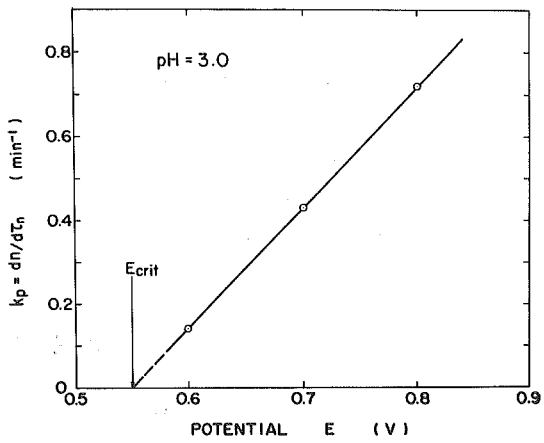

Fig. 11.

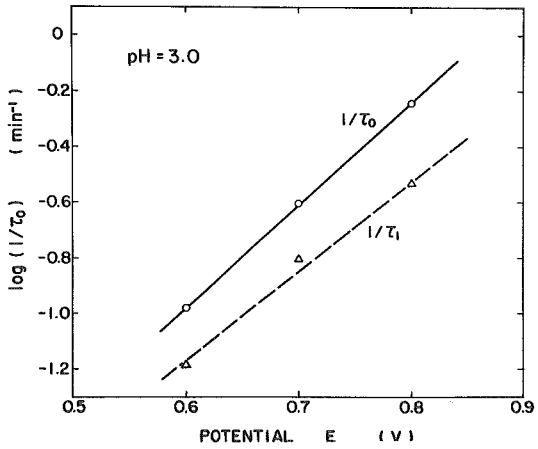

Fig. 12.

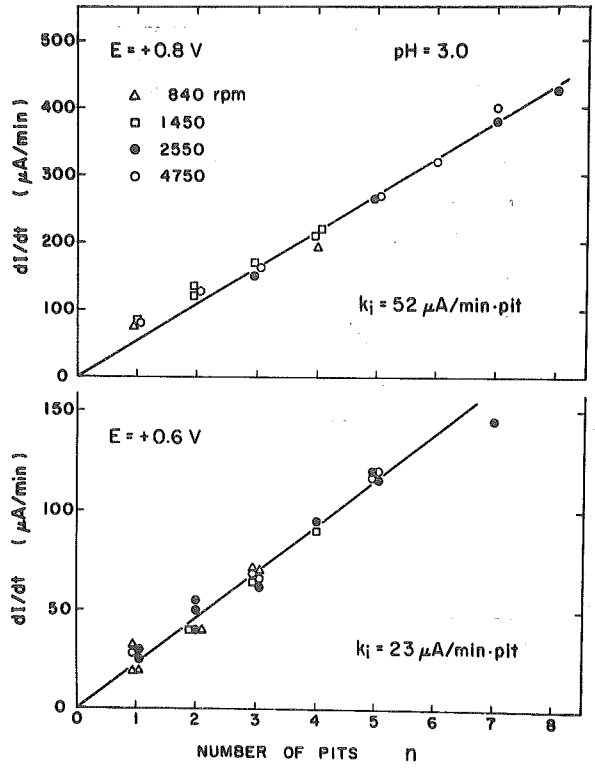

Fig. 13.

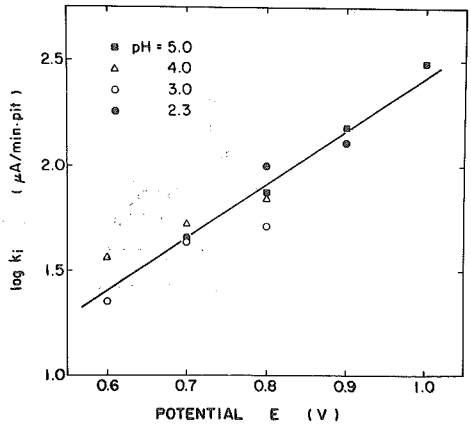

Fig. 14.

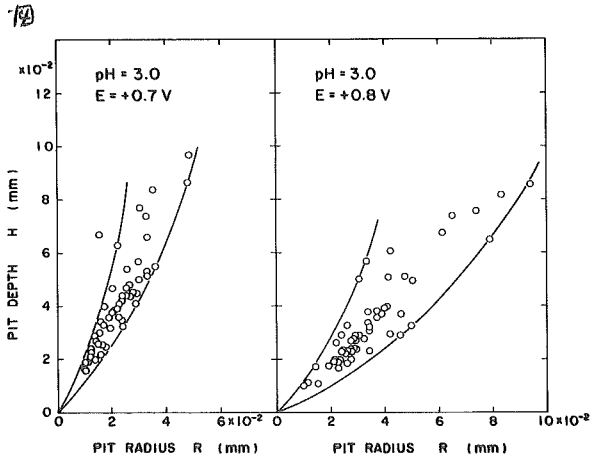

Fig. 15.

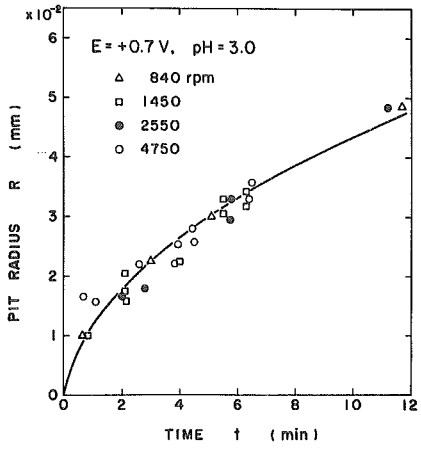

Fig. 16.

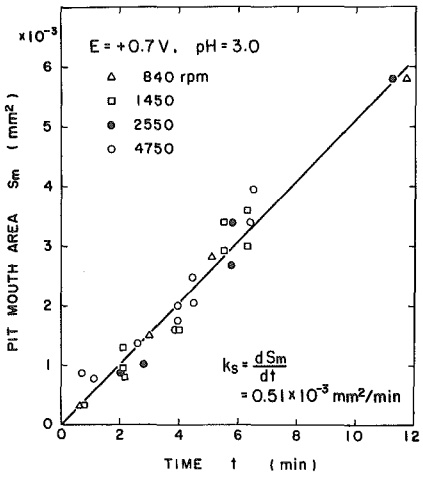

Fig. 17.

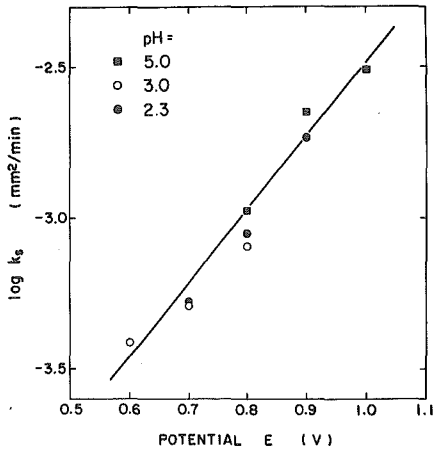

Fig. 18.

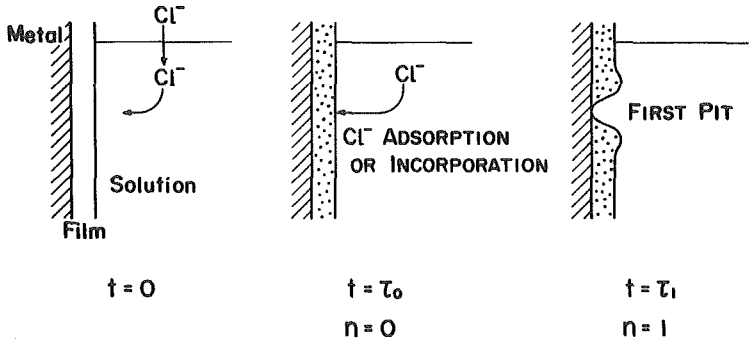

Fig. 19.

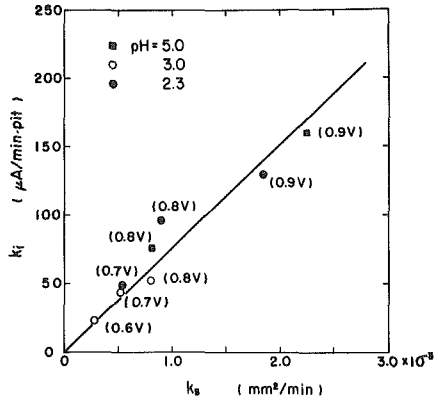

Fig. 20.

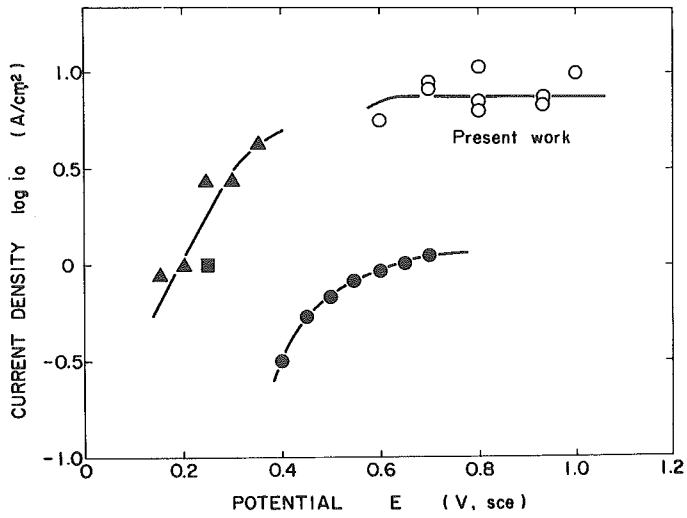
CURRENT DENSITY log io (A/cm²)
1.0
0.5
0
-0.5
-1.0
0
0.2
0.4
0.6
0.8
1.0
1.2
POTENTIAL E (V, sce)
Present work

Fig. 21.

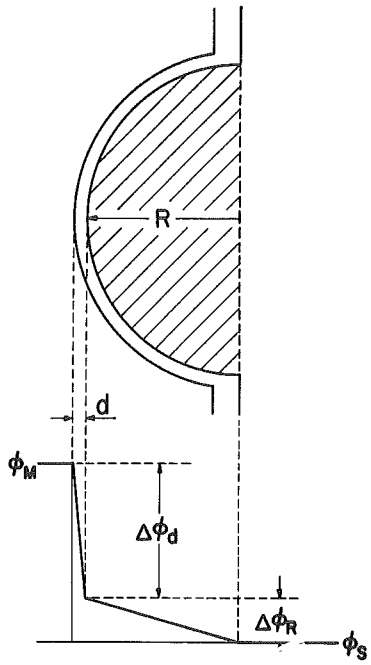
R
d
ϕ_M
$\Delta\phi_d$
$\Delta\phi_R$
ϕ_S

Fig. 22

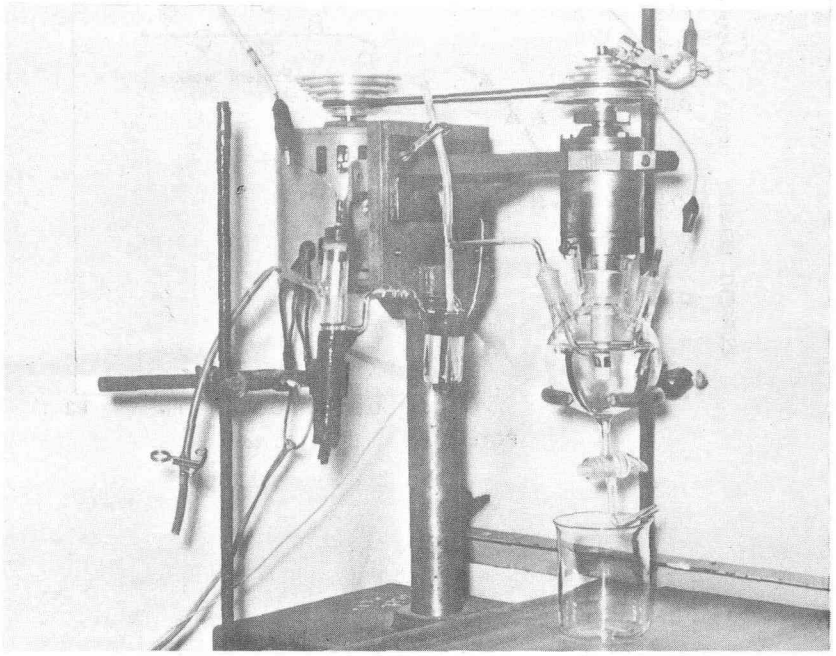

Photo 1.

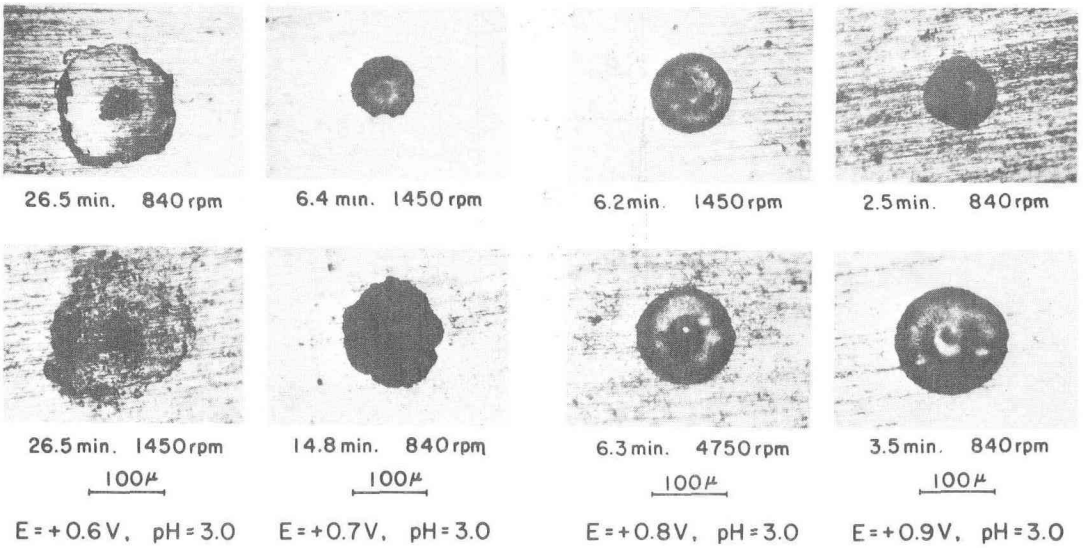

Photo 2.

Photo 3.

Table 1.

POTENTIAL (V)	SOLUTION pH	$k_i = d(dI/dt)/dn$ (μA/min·pit)	$k_S = dS_m/dt$ (mm²/min)	i_o (A/cm²)
1.0	5.0	305	3.10×10^{-3}	9.83
0.9	5.0	150	2.25	6.68
	2.3	131	1.85	7.08
0.8	5.0	76.5	1.05	7.28
	4.0	72.0		
	3.0	52.0	0.80	6.50
	2.3	100	0.90	11.1
0.7	4.0	54.0		
	3.0	43.6	0.51	8.46
	2.3	46.0	0.52	8.84
0.6	4.0	37.0		
	3.0	23.0	0.39	5.90